Quantitative Analysis of "Polymer-Balls" in Aqueous Solutions by Small-Angle Neutron Scattering

Mitsuhiro Shibayama*, Satoshi Okabe, and Michihiro Nagao

Neutron Scattering Laboratory, Institute for Solid State Physics, University of Tokyo, Tokai, Ibaraki, 319-1106, Japan

Shinji Sugihara and Sadahito Aoshima

Department of Macromolecular Science, Graduate School of Science, Osaka University, Toyonaka, Osaka 560-0043, Japan

Tamotsu Harada and Hideki Matsuoka

Department of Polymer Chemistry, Graduate School of Engineering, Kyoto University, Kyoto 606-8501, Japan

Abstract: The quantitative analysis of polymer micelles consisting of amphiphilic block copolymers was carried out by small-angle neutron scattering (SANS). The block copolymers, made of poly(2-ethoxyethyl vinyl ether-*b*-2-hydroxyethyl vinyl ether) (poly(EOVE-*b*-HOVE)), exhibited a sharp morphological transition from a homogeneous solution to a micelle structure with increasing temperature. This transition is accompanied by a formation of spherical domains of poly(EOVE) with a radius around 200 Å. The variations of the size and its distribution of the domains were investigated as a function of polymer concentration and temperature. The validity of SANS analysis, including the wavelength- and incident-beam-smearing effects of the SANS instrument, was examined with a pre-calibrated polystyrene latex.

Keywords: SANS, block copolymers, poly(EOVE-*b*-HOVE), micelle, morphological transition.

Introduction

Block copolymers have long been recognized as typical systems capable of self-assembling, particularly in the last several decades.[1,2] The most characteristic feature of block copolymers lies in the presence of chemical junction connecting unlike polymer chains, which results in a nanometer-order phase separation, the so-called microphase separation. The microphase separation is governed by the molecular weights, composition, the interaction parameter of the constituent blocks, and polymer concentration if the block copolymer is in a solvent.[3] Recently, studies on ordering and/or morphological transitions of block copolymers in a selective solvent have been extensively carried out.[4-7] These transitions are ascribed to the temperature and/or concentration dependence of the van der Waals interaction between the polymer chain and solvent.

An amphiphilic block copolymer consisting of hydrophilic and hydrophobic block copolymer chains is expected to undergo micellization in water, where hydrophobic interaction plays a major role in controlling the morphology.[8,9] Aoshima *et al.* prepared a series of stimuli-responsive block copolymers with polyalcohol branches[10] and vinyl ether segments in the side group.[11-13] Because of a narrow molecular weight distribution, a sharp transition in turbidity as well as in viscosity with respect to temperature was observed. Here, poly(2-ethoxyethyl vinyl ether-*b*-2-hydroxyethyl vinyl ether) (poly(EOVE-*b*-HOVE)) aqueous solutions were chosen to study the mechanism of micelle formation upon an increase of temperature.

In this paper, we carried out a microscopic investigation of poly(EOVE-*b*-HOVE) with small-angle neutron scattering (SANS) obtained with the small-angle neutron scattering instrument of The University of Tokyo, SANS-U. The performance of SANS-U will be also examined with a quantitative analysis of the size and size-distribution on pre-calibrated model sphere, polystyrene latex.

Theoretical Background

The form factor for a sphere is given by $\Phi^2(q)$, where

$$\Phi(qR) = \frac{3[sin(qR) - qRcos(qR)]}{(qR)^3} \equiv 3\sqrt{\frac{\pi}{2}} \frac{J_{3/2}(qR)}{(qR)^{3/2}} \quad (1)$$

Here, R is the radius of the sphere and $\Phi(x)$ is related to the Bessel Function of the order of 3/2, i.e., $J_{3/2}(x)$. q is the momentum transfer defined by

$$q = \frac{4\pi}{\lambda} sin\theta \quad (2)$$

where λ is the wavelength of the incident beam and θ is the scattering angle. The SANS intensity function for an assembly of dispersed spheres is given by

$$I(q) = nV^2(\Delta\rho)^2 \Phi^2(qR) \quad (3)$$

where n is the number of spheres in the unit volume (e.g., cm^3), V is the volume of the sphere, and $\Delta\rho$ is the scattering-length density difference between the particle (p) and the solvent (s), given by

$$\Delta\rho = \rho_p - \rho_s \quad (4)$$

The scattering-length density is evaluated by the following equation

$$\rho_i \equiv \frac{b_i}{v_i} = \frac{b_i}{m_i/d_iN_{AV}} \quad (5)$$

where b_i, v_i, m_i, and d_i are the scattering length, segment molar volume, molecular mass, and the mass density of the component i, respectively. N_{AV} is the Avogadro's number. Hence, the number density, n, is related to the weight fraction of the spheres,

$$n = \frac{w}{d_pV} \quad (6)$$

the scattering intensity is given by

$$I(q) = \frac{w}{d_p}V(\rho_p - \rho_s)^2 \Phi^2(qR) \quad (7)$$

In reality, in order to conduct a curve fitting of the scattering intensity functions, one needs to take account of several factors; (i) size distribution of spheres, (ii) wavelength distribution of the incident neutron beam, and (iii) the instrumental smearing due to a finite size of incident beam. The size distribution, $W_R(R)$, can be assumed to be a Gaussian function given by

$$W_R(R) \sim exp\left[-\frac{(R - \langle R \rangle)^2}{2(\Delta R)^2}\right] \quad (8)$$

where $\langle R \rangle$ is the average radius of the sphere and ΔR is the standard deviation of the radius. Hence eq (7) has to be rewritten to[14]

$$I_R(q) = \langle n \rangle \Delta\rho^2 \frac{\int W(R)V^2(R)\Phi^2(qR)dR}{\int W(R)dR} \quad (9)$$

Here, $\langle n \rangle$ is the average number of spheres in the unit volume and is given by

$$\langle n \rangle = \frac{w}{d_p\langle V \rangle} = \frac{\int W(R)dR}{\int W(R)VdR} \quad (10)$$

One can assume a Gaussian distribution for the wavelength distribution, $W_\lambda(\lambda)$, with

$$W_\lambda(\lambda) \sim exp\left[-\frac{(\lambda - \langle \lambda \rangle)^2}{2\sigma^2_\lambda}\right], \sigma_\lambda = FWHM/2\sqrt{2ln2} \quad (11)$$

where FWHM is the full-width at half maximum. Then, the corrected intensity, $I_{R+\lambda}(q)$, is given in the following form,

$$I_{R+\lambda}(q) = \frac{w}{d_p}\Delta\rho^2 \frac{\int\int W_R(R)W_\lambda(\lambda)V^2(R)\Phi^2(qR)dRd\lambda}{\int\int W_R(R)W_\lambda(\lambda)V(R)dRd\lambda} \quad (12)$$

Note that the effect of the wavelength distribution becomes larger with increasing q due to the following relationship,

$$dq = -\frac{4\pi}{\lambda^2}sin\theta d\lambda = -q\frac{d\lambda}{\lambda} \quad (13)$$

The effect of incident-beam smearing was also taken into account by convoluting $I(q)$ with the incident beam profile function at the detector plane. The coordinate is shown in Figure 1. The smeared intensity is given by

$$\tilde{I}(q) = \frac{2\int\limits_{p=0}^{p_m}\int\limits_{\alpha=0}^{\pi} I(\sqrt{(q-pcos\alpha)^2 + p^2sin^2\alpha})pdpd\alpha}{2\int\limits_{p=0}^{p_m}\int\limits_{\alpha=0}^{\pi} pdpd\alpha}$$

$$= \frac{2\int\limits_{p=0}^{p_m}\int\limits_{\alpha=0}^{\pi} I(\sqrt{(q-pcos\alpha)^2 + p^2sin^2\alpha})pdpd\alpha}{2 \cdot \frac{1}{2}p_m^2\pi} \quad (14)$$

$$= \frac{2}{\pi p_m^2}\int\limits_{p=0}^{p_m}\int\limits_{\alpha=0}^{\pi} I(\sqrt{(q-pcos\alpha)^2 + p^2sin^2\alpha})pdpd\alpha$$

Experimental

Sample. An amphiphilic block copolymer, poly(2-ethoxyethyl vinyl ether-*b*-2-hydroxyethyl vinyl ether), poly(EOVE
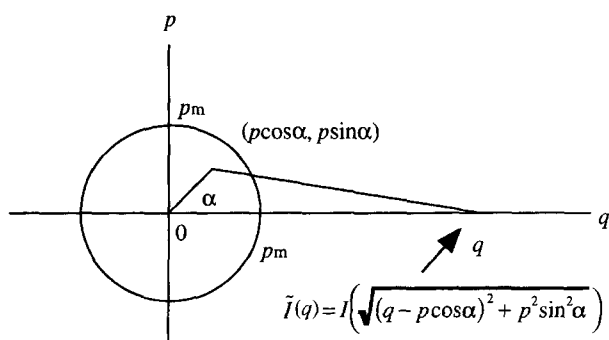
Figure 1. Definition of the coordinate on the detector plane.

-*b*-HOVE), was polymerized by living cationic polymerization. The details of sample preparation are reported elsewhere.[15] Poly(EOVE-*b*-HOVE) has the number average molecular weight of $\overline{M_n}$ = 5.84 × 10^4, and the polydispersity index of $\overline{M_w}/\overline{M_n}$ = 1.07. The degrees of polymerization of EOVE and HOVE were evaluated to be 200 and 400, respectively. Polystyrene (PS) latices were synthesized by emulsifier-free emulsion polymerization of styrene and divinylbenzene in the presence of potassium styrenesulfonate with potassium persulfate as an initiator. The sample codes are 153H, 155H, 155D, and 157D, where H and D denote the solvents, namely H for H_2O and D for D_2O. The radius of the spheres, *R*, and size-distribution of these PS spheres in powder state are determined to be 530 Å (0.12), 540 Å (0.10), and 650 Å (0.06), for latices 153, 155, and 157, respectively, by ultra small-angle X-ray scattering (USAXS),[16,17] where the numbers in the parenthesis indicates the standard deviation of the spheres normalized to *R*, $\Delta R/<R>$.[18] The concentration of the polystyrene was 1 vol%.

SANS. Small-angle neutron scattering (SANS) experiment was carried out at the SANS-U spectrometer, Institute for Solid State Physics, The Univ. of Tokyo.[19] Cold neutrons from the JRR-3M research reactor of Japan Atomic Energy Research Institute, Tokai, Ibaraki, Japan, were monochromatized to a $<\lambda>$ = 7.0 Å beam with a neutron velocity selector, where $<\lambda>$ the average wavelength. The wavelength distribution FWHM was 13%. The sample-to-detector distance (SDD) was varied from 2 to 4, 8, and 12 m. The temperature of the sample was regulated with a water-circulating bath (NESLAB RTE-111M). Samples in quartz cells of 1 mm-thick (for PS latex) or 4 mm-thick (for poly(EOVE-*b*-HOVE) aqueous solutions) were irradiated by the neutron beam for 30 or 60 min depending on the scattering power. The scattered intensity functions were corrected for transmission, and air scattering, and then circularly averaged. The subsequent absolute intensity calibration was carried out with the incoherent scattering from a Lupolen® (polyethylene) secondary standard sample.[20]

Results and Discussion

Performance of the SANS-U. Figure 2 shows the optical setup of the SANS-U, which is characteristic of its symmetrical setup of the incidence and the scattering geometry. This allows one to optimize the neutron flux and the spatial resolution for a given SDD. For example, the illuminated area on the detector plane is independent of SDD as shown in the figure for the cases of SDD = 4 and 8 m. The observed profile of the incident beam is shown in Figure 3 for the case of sample aperture size being 5 mm. Since the pixel size is 5 mm, the FWHM is calculated to be 4 pixels irrespective of the collimation condition. This corresponds to FWHM = 2.24 × 10^{-3} Å^{-1}. This is in good accordance with the observed profile, $W_{inc}(q)$, of which FWHM ≈ 2.34 × 10^{-3} Å^{-1}.

Figure 4 shows the incoherent scattering from Lupolen®. The relative intensity difference between different collimation

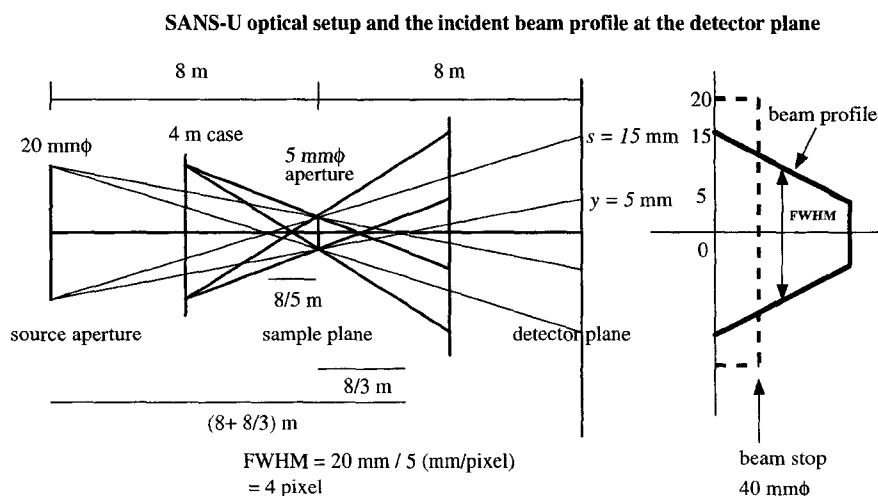**SANS-U optical setup and the incident beam profile at the detector plane**

Figure 2. Optical setup of the Tokyo University SANS instrument, SANS-U, showing the symmetric neutron path and the beam profile at the detector plane.
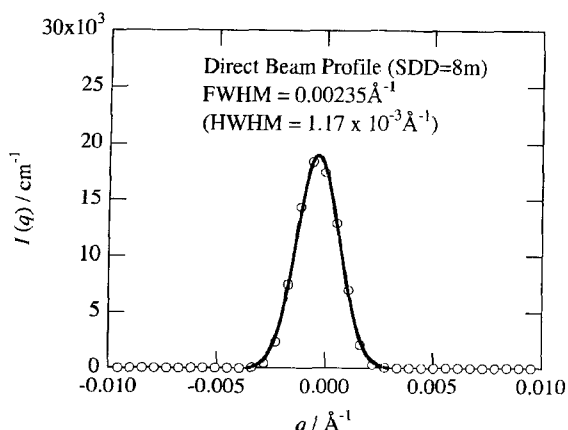
Figure 3. Observed direct beam profile with the condition of 8 m collimation, 8 m SDD, and 5 mm sample aperture.
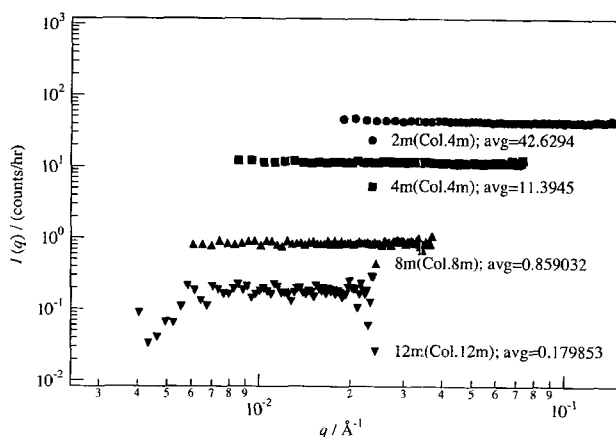

Figure 4. Scattering intensity function from Lupolen® observed at various optical conditions. The numbers outside and inside the parenthesis indicates the sample-to-detector distance (SDD) and the collimation length, respectively. The numbers following "avg" mean the relative ratios of the intensity among different geometries.

Figure 5. Examples of curve fitting results, i.e., polystyrene latex ("polyball") 157D: (a) the effect of particle size distribution; (b) the effects of instrumental smearing.

conditions is also given as the "avg". The attainable minimum q is estimated to be 0.003 Å^{-1} for SDD = 12 m, and 0.005 Å^{-1} for SDD = 8 m, and 0.008 Å^{-1} for SDD = 4 m. It should be noted here the subtraction of air scattering was too large for the case of SDD = 12 m due probably to a slight over-estimation of the transmittance, resulting in a dip in the scattering intensity from a constant value for $q < 0.006$ Å^{-1}. This seems to be an artifact because the result for PS latex does not show any anomaly down to $q = 0.003$ Å^{-1} as will be shown in Figure 6.

Examination of the Curve Fitting Procedure with PS Latex. Figure 5(a) shows the results of curve fitting for 157D, where the distribution of the radius of the spheres is taken into account. This clearly shows significant smearing occurs due to the size distribution. Although smearing effects
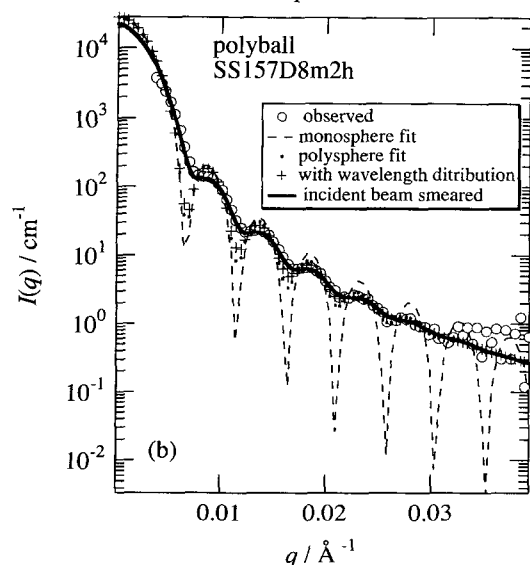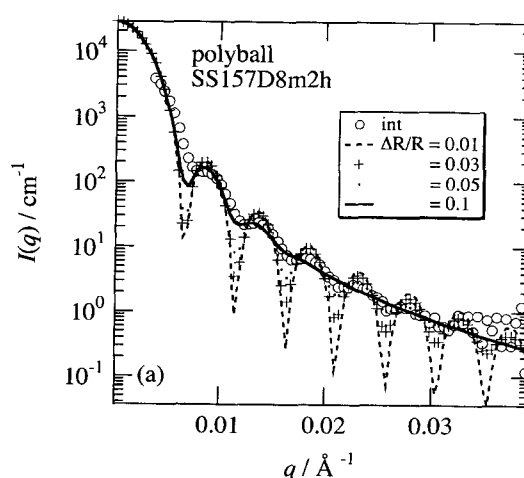
have to be taken into account for more precise fitting, the distribution was estimated to be $\Delta R/<R> \approx 0.1$ with eqs (8) and (9). Figure 5(b) shows the effects of polydispersity of particle size, wavelength distribution, and incident-beam smearing. For calculation, the value of 2.34 × 10^{-3} Å^{-1} was used for the width of the incident beam. The fitting result indicates that the incident-beam smearing is more significant than the effect of wavelength distribution.

Figure 6 shows the results of curve fitting for scattering intensity functions for 157D obtained with different SDDs, i.e., 4, 8, and 12 m. The effect of spatial resolution and the lower bound of accessible q are clear. It seems to be relevant to choose SDD = 12 m for this system. The average size, $<R>$, and its distribution, $\Delta R/<R>$, are respectively evaluated to be 650 Å and 0.06 by USAXS. Hence, the agreement of the SANS and USAXS results seem to be reasonable, which
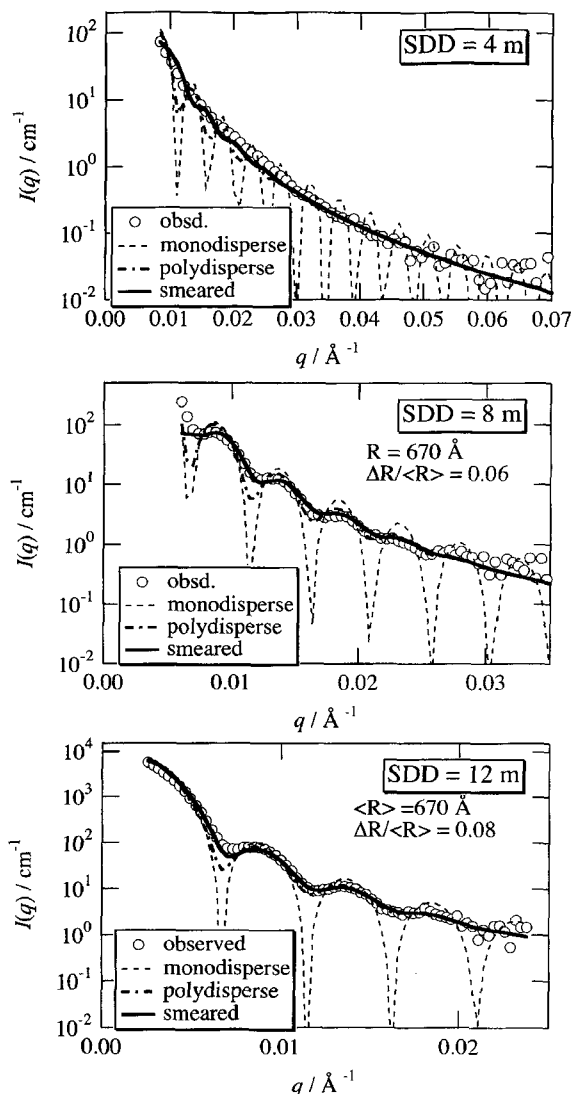
Figure 6. Comparison of scattering intensity curves for 157D obtained with different geometries and the results of curve fitting.

guarantees the validity of the SANS analysis.

Analysis of the Structure of Thermosensitive Block Copolymer Micelles. Figure 7 shows the SANS intensity functions of poly(EOVE-b-HOVE) aqueous solutions at various temperatures. The concentrations were 2 to 17 wt%. At temperature $T = 15$ and $17\,°C$, $I(q)$ are monotonically decreasing functions with q. However, $I(q)$ drastically changes between 17 and $19\,°C$, and increases remarkably with further increasing temperature. $I(q)$ exhibits several scattering maxima, indicating appearance of spherical domains as discussed in the previous section. Remarkable change in flow behavior around this transition temperature was also observed.[15] The storage modulus increased by the factor of 4 within the temperature range between 19 and $20\,°C$.

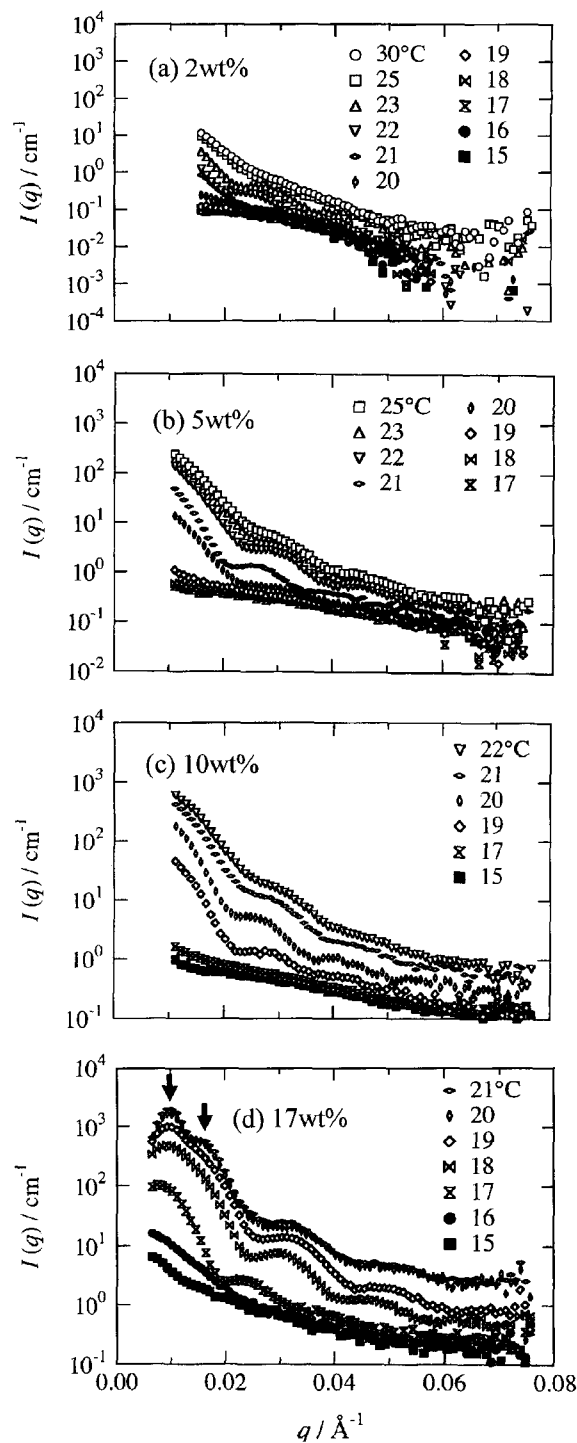Quantitative analysis was conducted for the thermosensi-

Figure 7. Scattering intensity functions for poly(EOVE-b-HOVE) observed at various temperatures.

tive block copolymers with polymer concentration $C = 17$ wt% with the curve fitting method discussed in the previous section. The results are shown in Figure 8, and a good fitting was attained with reasonable fitting parameters. Curve fitting
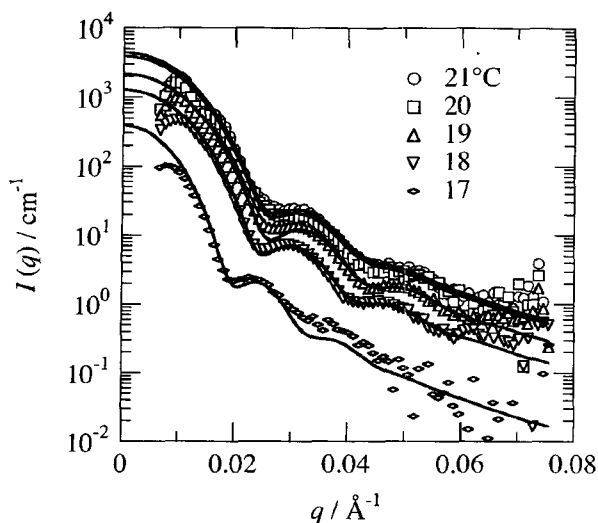
Figure 8. Results of curve fitting for $I(q)$ of poly(EOVE-*b*-HOVE). The open circles are the observed data and the solid lines indicate the fitting results.
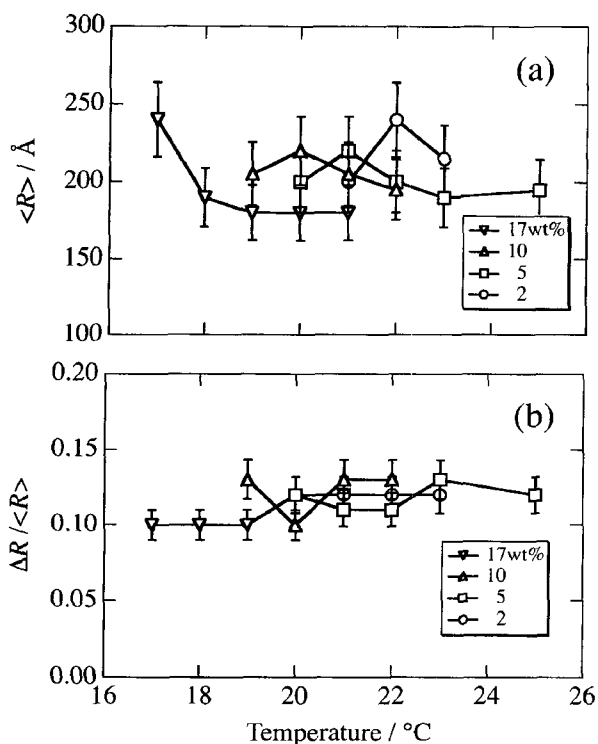

Figure 9. Temperature dependence of the size <*R*> and size-size distribution, $\Delta R/<R>$, of poly(EOVE-*b*-HOVE) at various concentrations.

for other SANS functions for the thermosensitive polymers with different concentrations were also taken and a similar behavior was obtained. Figure 9 shows the variation of the average radius, <*R*> and radius distribution, $\Delta R/<R>$, with

concentration and temperature obtained by curve fitting. Interestingly, the size and its distribution are little dependent on polymer concentration and temperature.

The temperature independence is due to strong temperature dependence of hydrophobic interaction. That is an all-or-none type interaction due to melting/forming of iceberg structure.[21-23] In the case of a van der Waals interacting system, such as block copolymers in an organic solvent, the interaction parameter between polymer chains and the solvent varies continuously with temperature. On the other hand, a hydrophobically interacting system undergoes a sharp transition from miscible to phase separating system upon a slight temperature change. The concentration independence comes from thermodynamic requirement of block copolymers to form a unique size of microdomains.[2] That is, the domain size is a strong function of the molecular weight of the block chains M, e.g., $R \sim M^{2/3}$, as is extensively discussed in the theories of block copolymers.[2] More detailed studies including analysis of inter-particle interference are discussed elsewhere.[15]

Conclusions

Nano-order structure formation of block copolymers (poly(EOVE-*b*-HOVE)) in aqueous systems has been quantitatively studied by SANS. First, the validity of the SANS analysis was carefully examined with pre-calibrated polystyrene latex from the viewpoints of size distribution of domains and instrumental smearing effects. It was found that the incident-beam smearing effect is dominant over the wavelength-distribution effect in this particular case. In the micelle regime, the size of core is about 200 Å and is hardly dependent on either temperature or polymer concentration. These facts clearly indicate two important features of amphiphilic block copolymer aqueous systems. Those are (i) presence of a all-or-none type interaction between poly(EOVE) and water due to melting/forming of iceberg structure, and (ii) strong thermodynamic requirement of block copolymer to form microdomains with a unique size.

References

(1) G. E. Molau, in *Block Polymers*, S. L. Aggarwal, Ed., Plenum Press, N.Y., 1970.
(2) E. Helfand and Z. R. Wasserman, in *Developments in Block Copolymers*, I. Goodman, Ed., Applied Science, New York, 1982.

(3) M. Shibayama, T. Hashimoto, and H. Kawai, *Macromolecules*, **16**, 1093 (1983).

(4) G. A. McConnell and A. P. Gast, *Macromolecules*, **30**, 435 (1997).

(5) G. A. McConnell, A. P. Gast, J. S. Huang, and S. D. Smith, *Phys. Rev. Lett.*, **71**, 2102 (1993).

(6) C. I. Huang and T. P. Lodge, *Macromolecules*, **31**, 3556 (1998).

(7) K. J. Hamley, T. P. Lodge, and C. I. Huang, *Macromolecules*, **33**, 5918 (2000).

(8) L. Zhang and A. Eisenberg, *Science*, **268**, 1728 (1995).

(9) P. Alexandridis, U. Ollson, and B. Lindman, *Langmuir*, **14**, 2627 (1998).

(10) S. Aoshima and K. Hashimoto, *J. Polym. Sci., Polym. Chem. Ed.*, **39**, 746 (2001).

(11) S. Aoshima and S. Sugihara, *J. Polym. Sci., Polym. Chem. Ed.*, **38**, 3962 (2000).

(12) S. Sugihara and S. Aoshima, *Koubunshi Ronbunshu*, **58**, 304 (2001).

(13) S. Sugihara, S. Matsuzono, H. Sakai, M. Abe, and S. Aoshima, *J. Polym. Sci., Polym. Chem. Ed.*, **39**, 3190 (2001).

(14) H. Hashimoto, M. Fujimura, T. Hashimoto, and H. Kawai, *Macromolecules*, **14**, 844 (1981).

(15) S. Okabe, S. Sugihara, S. Aoshima, and M. Shibayama, *Macrmolecules*, **35**, 8139 (2002).

(16) H. Matsuoka, K. Kakigami, N. Ise, Y. Kobayashi, Y. Machitani, T. Kikuchi, and T. Kato, *Proc. Natl. Acad. Sci. USA*, **88**, 6618 (1991).

(17) H. Matsuoka and N. Ise, *Chemtract*, **4**, 53 (1993).

(18) M. Nagao, S. Okabe, M. Shibayama, and H. Matsuoka, *Activity Report on Neutron Scattering Res.*, **8**, 39 (2001).

(19) Y. Ito, M. Imai, and S. Takahashi, *Physica B*, **213 & 214**, 889 (1995).

(20) D. Schwahn, H. Takeno, L. Willner, H. Hasegawa, H. Jinnai, T. Hashimoto, and M. Imai, *Phys. Rev. Lett.*, **73**, 3427 (1994).

(21) B. Alberts, D. Bray, J. Lewis, M. Raff, K. Roberts, and J. D. Watson, *Molecular Biology of the Cell*, Garland Publishing Inc., New York, 1994.

(22) M. Shibayama, M. Morimoto, and S. Nomura, *Macromolecules*, **27**, 5060 (1994).

(23) M. Shibayama, S. Mizutani, and S. Nomura, *Macromolecules*, **29**, 2019 (1996).